The M6.4 Lefkada 2003, Greece, earthquake: dynamic response of a 3-storey R/C structure on soft soil

Christos Giarlelis*, Despina Lekka, George Mylonakis and Dimitris L. Karabalis

Department of Civil Engineering, University of Patras, 26504 Rio, Greece

Abstract. An evaluation is presented of the response of a 3-storey R/C structure during the destructive Lefkada earthquake of 14/08/2003. Key aspects of the event include: (1) the unusually strong levels of ground motion (PGA = 0.48 g, SA_{max} = 2.2 g) recorded approximately 10 km from fault, in downtown Lefkada; (2) the surprisingly low structural damage in the area; (3) the very soft soil conditions ($V_{s,max}$ = 150 m/s). Structural, geotechnical and seismological aspects of the earthquake are discussed. The study focuses on a 3-storey building, an elongated structure of rectangular plan supported on strip footings, that suffered severe column damage in the longitudinal direction, yet minor damage in the transverse one. Detailed spectral and time-history analyses highlight the interplay of soil, foundation and superstructure in modifying seismic demand in the two orthogonal directions of the building. It is shown that soil-structure interaction may affect inelastic seismic response and alter the dynamic behavior even for relatively flexible systems such as the structure at hand.

Keywords: 2003 Lefkada earthquake; soft soil; soil-structure interaction; pushover analysis; inelastic seismic response.

1. Introduction

The earthquake occurred at 08:15am (05:15 UTC) August 14, 2003, with an estimated magnitude M_w = 6.2 (M_s = 6.4) and a seismic moment of approximately 2×10^{18} Nm, (Table 1). The source was located on several segments of a known dextral fault zone (approx. 14 degrees striking, 80 dipping), 130 km long and 30 km deep, running parallel to the west shore of the island (Fig. 1). Reconnaissance reports and engineering investigations have been published, among others, by Margaris *et al*. (2003), Bouckovalas and Papadimitriou (2003), Papadopoulos *et al*. (2003), Gazetas (2004), Karakostas *et al*. (2004, 2005), ITSAK (2004) and Sextos *et al*. (2010).

The losses induced by the earthquake were surprising low: no lives lost, less than 50 injured, one building collapse and a handful of R/C buildings damaged beyond repair. Most of the damage was limited to non-structural elements, such as masonry and roof tiles. On the other hand, geotechnical damage was much more pronounced, for extensive rockfalls occurred on the west part of the island, while quay walls in virtually all ports suffered considerable displacements.

After a brief discussion of certain geotechnical and seismological aspects of the earthquake, the study focuses on the dynamic behavior of structures in the area. Initially a ductility demand index is

---

* Corresponding author, Ph.D. Candidate, E-mail: giarlelis@alumni.rice.edu

Table 1 Source parameters

Source	M_w	M_s	Moment (Nm)	h (km)	Strike (deg)	Dip (deg)	Latitude (deg)	Longitude (deg)
USGS	6.2	-	2×10^{18}	10	13	84	39.18	20.74
Harvard	6.3	-	2×10^{18}	15	18	59	38.70	20.67
NOA	6.2	6.4	-	12	-	-	38.81	20.56
AUT	-	6.3	-	10	11[†]	60[†]	39.16	20.605
Zahradnik *et al.* (2003)*	6.2	-	2×10^{18}	10	19	83	38.79	20.56
					26	84	38.46	20.5

[†]data from Papazachos *et al.* (1998)
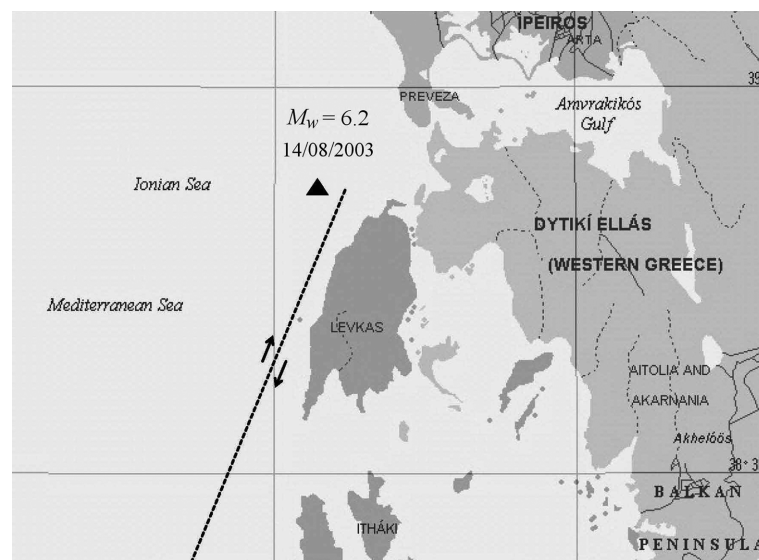*simulation (double values refer to different sub-events)

Fig. 1 Rough map of region showing fault and main event

evaluated for a SDF oscillator using non-linear time-history analysis; it is demonstrated why most structures survived the shaking almost undamaged. Then the dynamic behavior of a building that suffered severe damage is investigated. The building was selected for the simplicity of its structural system and is used as a case study to examine the role of various structural and geotechnical parameters on its dynamic response, and to show that the observed damage is consistent with the level and frequency content of seismic input.

2. Historical evidence

The earthquake did not come as a surprise: there is ample historical evidence (Table 2) of over a dozen earthquake-induced destructions in Lefkada during the past four centuries (Papazachos & Papazachos 1997). Available information suggests that 4 to 5 events above M 6¼ are released per century. This is also true for the past century, during which five strong events took place (1914,

Table 2 Destructive earthquakes in Lefkada in the period 1577 - 2003 A.D. (sources: Papazachos *et al.* 2003, Rondoyannis 1997, Spyropoulos 1997)

Location/ Year	Magnitude	Maximum intensity	Losses
Lefkada 2003	6.4	IX	No lives lost, 50 injured, one collapse, 5 R/C buildings damaged beyond repair, serious damages in masonry structures and in the ports of the capital and Lygia; Falling of rocks
Lefkada 1973	5.8	VII	Serious damages in the town of Lefkada
Vasiliki 1948	6.5	IX	11 dead, 244 collapses, serious damage in Vassiliki, Kalamitsi, Ag. Petros, Eglouvi; falling of rocks
Komilio 1914	6.3	IX	16 dead, destruction of 18 villages, subsidence of Nydri port, rock falls, settlement at Kalamitsi
Lefkada 1869	6.4	X	15 dead, destruction of villages Amaxiki and Tsoukalades
Lefkada 1825	6.5	X	58 dead, destruction of the capital and several villages
Lefkada 1820	6.4	IX	Extensive damage in the capital, ground settlement in the central square
Lefkada 1815	6.3	VIII	20 dead, destruction throughout the island
Athani 1783	6.7	X	10 dead, 862 collapses throughout the island, destruction of the village Athani, extensive damage in 10 other villages
Lefkada 1769	6.7	IX	7 dead, 497 collapses out of a total of 826 houses in the capital
Lefkada 1723	6.7	VIII	Significant damage in the island, especially in the capital
Athani 1722	6.4	VIII	Extensive collapses in Athani, Damiliani, Agios Petros, Agia Marina; serious damage in the castles of Agia Mavra and Aepetron
Lefkada 1704	6.3	IX	34 dead, massive collapses in the city of Lefkada and at Fryni
Katouna 1630	6.7	IX	Collapses in the city of Lefkada and at Katouna; Falling of rocks and trees, cracks in the ground, notably in the south part of the island
Lefkada 1625	6.6	IX	Massive collapses of masonry structures in the city
Lefkada 1613	6.4	VIII	Destruction of houses, palaces and minarets in the city of Lefkada, collapses throughout the island
Lefkada 1612	6.5	VIII	Damage in 4 villages
Lefkada 1577	6.2	VIII	Damage to the city walls

1948a, 1948b, 1978, 2003). Of interest is the occurrence of some double events (e.g. 1612-13, 1722-23, 1948a, 1948b) striking in the north and south parts of the island, respectively.

The earthquake at hand may also classify as a double event, as the rupture stopped close to Porto Katsiki and, several seconds later, resurrected at the island of Cephalonia (Benetatos *et al.* 2005,

2007, Zahradnik *et al*. 2005), 50 km south of the epicenter. The stretching and segmentation of the source prolonged the duration of shaking, as will be shown later in this article.

3. Engineering characteristics of strong ground motion

The mainshock was recorded by seven triaxial digital accelerometers (Margaris *et al*. 2003). One instrument was installed at the basement of a two-storey hospital building (to be called hereafter Hospital Station) in downtown Lefkada, about 10 km from fault. It provided the strongest record of the earthquake, with peak acceleration on horizontal plane of 0.48 g. A number of strong motion stations (including two in the neighboring towns of Preveza and Argostoli) provided the attenuation characteristics presented in Fig. 2. It should be noted that the attenuation data plot higher than the mean curves from the Scarlatoudis *et al*. (2003) study.

The analyses reported in this work are based on the Hospital Station record (Fig. 3). Comparing the earthquake characteristics with other destructive Greek earthquakes (Table 3) leads to the following noteworthy observations (for a more complete discussion see Mavroeidis and Papageorgiou 2000, Giarlelis *et al*. 2003, Mylonakis *et al*. 2003, Gazetas 2004):

a. Peak ground acceleration (0.42 g & 0.34 g) in the two horizontal directions was unusually strong and has been exceeded in Greece only in the records of M5.8 Lefkada (1973) and M6.1 Aegion (1995) earthquakes
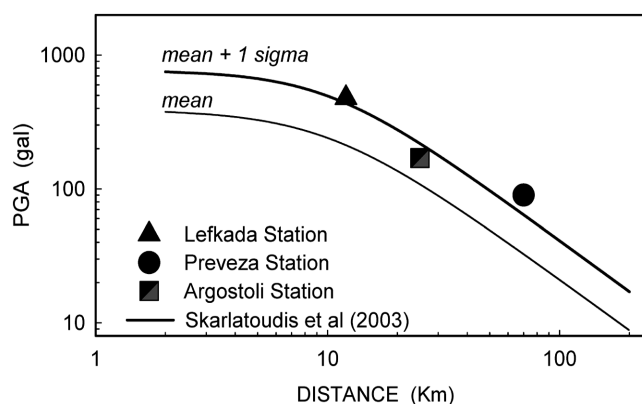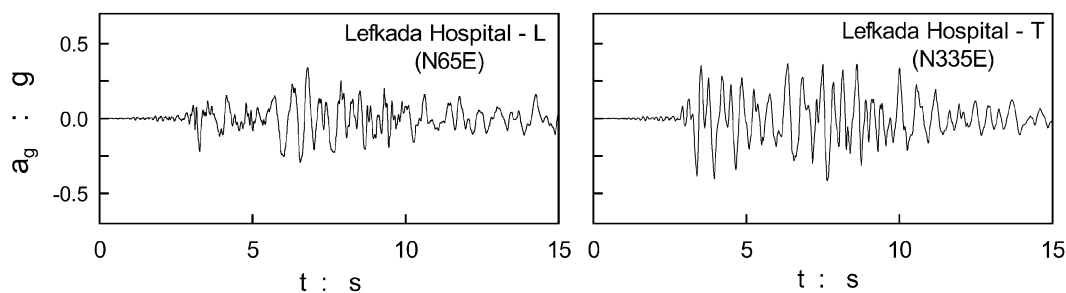

Fig. 2 Attenuation characteristics

Fig. 3 Time histories of horizontal accelerations recorded at the Hospital Station during the main event

Table 3 Peak values of recent strong ground motion recordings in Greece: peak ground acceleration (PGA), peak ground velocity (PGV), peak ground displacement (PGD), Housner Intensity (I_H), Arias Intensity (I_A), Bracketed Duration (D_B), Destructive Potential (D_p).

Station	Event/Date	Magnitude (M_s)	Epicentral distance (km)	Distance from fault (km)	Ground conditions	Instrument orientation		PGA (g)	PGV (cm/s)	PGD (cm)	I_H (cm)	I_A (m/s)	D_b (s)	D_P (cm/s^2)
Lefkada OTE	Ionian sea 11/04/1973	5.7	15	11	Soft	L	N-S	0.53	57.02	12.02	168.1	1.36	7.9	5.3
					Soil	T	E-W	0.26	25.51	4.77	76.8	0.5	8.4	1.7
Kalamata OTE	Kalamata 09/13/1986	5.8	10	5	Stiff	L	N80E	0.24	31.56	6.83	100.9	0.55	5.7	1.4
					Soil	T	N10W	0.27	23.59	5.18	89.8	0.74	8.0	2.0
Aegion OTE	Aegion 06/15/1995	6.2	18	4	Stiff	L	N-S	0.54	50.91	9.70	110.8	1.15	5.1	2.3
					Soil	T	E-W	0.49	39.77	6.90	116	0.98	6.3	1.2
Monastiraki METRO	Athens 07/09/1999	5.9	17	13	Stiff	L	N20	0.23	14.84	3.79	0.22	54.56	3.17	0.4
					Soil	T	N290	0.50	14.64	2.17	0.75	49.61	5.63	0.6
Sepolia METRO	Athens 07/09/1999	5.9	14	9	Stiff	L	N320	0.32	21.53	2.50	0.58	64.79	5.48	0.002
					Soil	T	N50	0.31	18.60	2.44	0.66	62.3	6.57	0.003
Lefkada OTE	Ionian sea 14/08/2003	6.4	14	14	Soft	L	N65E	0.34	28.4	-	129.1	2.03	15.2	5.1
					Soil	T	N335W	0.42	35.2	-	126.6	4.08	10.6	1.2

b. Housner Intensity

$$I_H = \int\limits_{0.2}^{2.5} SV\,dT = 129.2 \text{ cm} \tag{1}$$

is extremely large - indicative of high spectral velocity and has been exceeded only in the Lefkada record of 1973.

c. Arias Intensity

$$I_A = \frac{\pi}{2g} \int\limits_{0}^{t_d} \ddot{u}_g^2(t)\,dt = 4.08 \text{ m/s} \tag{2}$$

is by far the strongest ever recorded in Greece, indicative of large duration.

d. Bracketed Duration is, by Greek standards, unusually high, equal to 15.2 s, which has been exceeded only in the much bigger M6.7 Alkionides event of 1981. This value confirms the high intensity figures presented in Eqs. (1) and (2). It is worth mentioning that the bracketed duration is higher in the direction of smaller acceleration (N65E). The large duration is anticipated given the soft soil conditions, the extended-segmented seismic source and possible directivity effects, as discussed below.

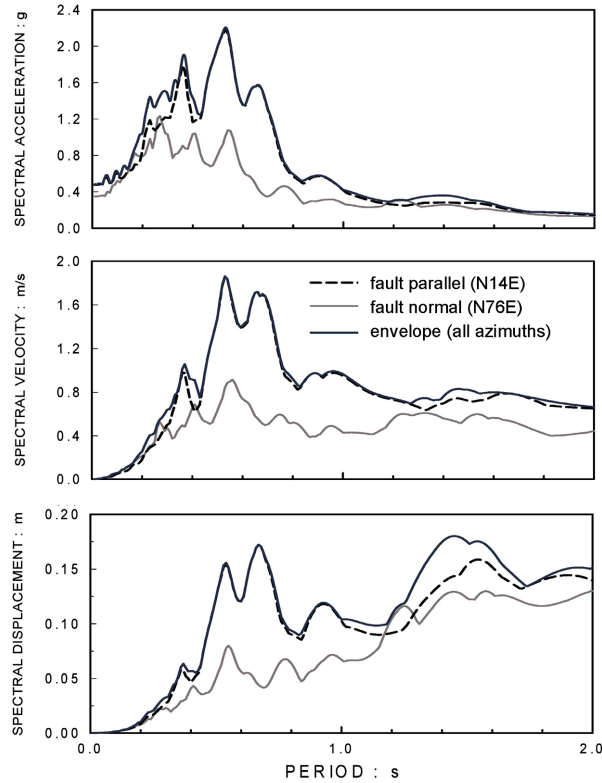Acceleration, velocity and displacement spectra of the Hospital motion are provided in Fig. 4.

Fig. 4 Response spectra from Hospital station record oriented at fault parallel and fault normal directions, $\xi = 5\%$.
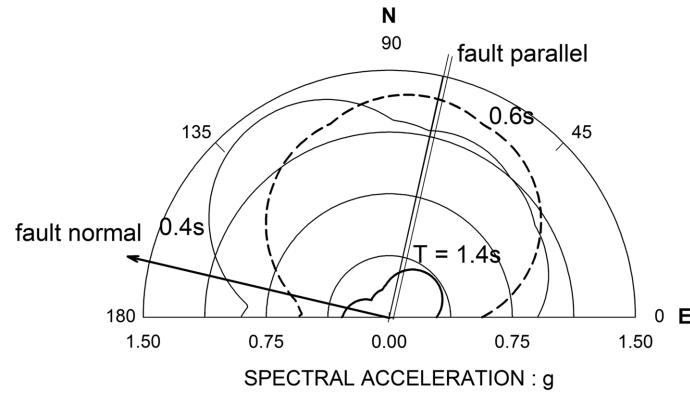
Fig. 5 Polar representation of spectral accelerations, from Hospital station record, at different periods, $\xi = 5\%$.

Values are plotted along the fault-normal direction, fault-parallel direction, and envelope for all orientations. It is observed that (Gazetas 2004, Giarlelis *et al*. 2006):

- Spectral accelerations exceed the remarkably high value of 2.2 g at 0.53 s, and drop significantly only after about 1s. These strong accelerations can be partially attributed to seismological factors (source effects), as well as geotechnical factors such as soil amplification (due to trapping of the up- and down- reflected seismic waves in the soft surface layer in the town of Lefkada).
- The predominant period of ground acceleration is approximately 0.55 s; the record is rich in periods as high as 0.7 s. These values are among the most severe ever recorded in Greece.
- Peak spectral velocity, 1.8 m/s at 0.5 s, is also remarkably high and provides indirect evidence of the significant sliding of rigid bodies observed in the town of Lefkada and elsewhere in the island.

Gazetas (2004) points out that the effective peak acceleration (i.e. average spectral values in the range from 0.2 s to 0.6 s over 2.5)

$$EPA = \frac{1}{0.6-0.2} \int_{0.2}^{0.6} SAdT \tag{3}$$

attains values over 0.55 g, the highest ever recorded in Greece. These values are about 50% higher than the one adopted in the current seismic code (OASP 2003) for the area (0.36 g). Also important are the high values of spectral displacements, which approach 18cm at long periods (Fig. 4). This is an important parameter which may affect the response of inelastic structures, as discussed later in this article.

Also of interest is the polar representation of SA values shown in Fig. 5, plotted as function of the azimuth angle for three different periods. The orientations of the fault trace and the normal direction are also shown. It is observed that: (1) at relatively long periods (0.6 s and 1.4 s), spectral values in the direction parallel to fault are significantly higher than those normal to fault. (2) In the shorter period of 0.4 s, spectral accelerations in the fault-normal and the fault-parallel directions are comparable in magnitude. For the particular source mechanism, and given the small distance from the fault, this behaviour could be attributed to backward directivity of the source (which may also be inferred from the time histories in Fig. 3).

4. Inelastic response: preliminary assessment

Information on the response of a yielding single-degree-of-freedom (SDOF) structure is provided from inelastic ductility spectra shown in Fig. 6. The associated parameters are the seismic yield coefficient

$$C_y = F_y / W \qquad (4)$$

and the post- yielding stiffness factor

$$\alpha = K_{py} / K \qquad (5)$$

where F_y και W denote the yield force capacity and weight of the structure, respectively; K_{py} and K are, respectively, the post-yield stiffness and elastic stiffness of a conceptual single-degree-of-freedom structure with bilinear force-displacement characteristics.

The above spectra have been evaluated for values of C_y ranging between 0.1 and 0.5 and $\alpha = 0.15$. The lower bound corresponds roughly to a structure designed for low levels of seismic excitation, whereas the upper bound to a structure designed according to the modern Greek seismic code (OASP 2003) for the area at hand. It is observed that ductility demand is higher in the direction parallel to fault as compared to that normal to fault.

As a first approximation, it is useful to evaluate the performance of a typical structure in the area in light of this information. Given that most structures in Lefkada suffered only minor damage, to limit the inelastic demand to less than approximately 2 according to the data of Fig. 6, requires

$$C_y > 0.5 \text{ and } T < 0.2 \text{ s} \qquad (6)$$

The above strength requirement is rather demanding, especially for old structures. A possible explanation is that the actual mass-normalized strength of traditional structures in the area (built using an ingenious combination of masonry and wood which minimizes mass) is unusually high; to the best of the authors' estimate, structures are, due to low weight, capable of resisting a normalized seismic shear 4 to 5 times higher than the design value specified in the 1959 Seismic code.
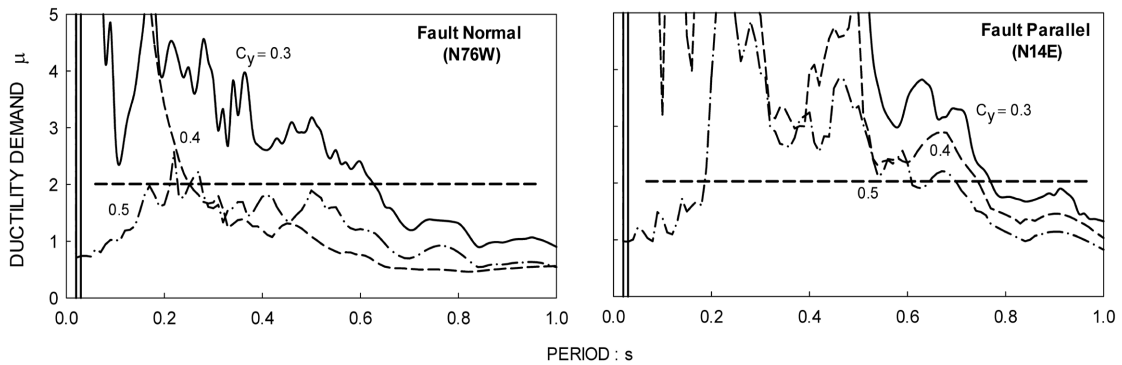
Fig. 6 Ductility spectra, from Lefkada Hospital record, at orientations normal and parallel to fault

Considering a value of $C_y* = 0.12$ as specified by that seismic code, in conjunction with the above overstrength, yields

$$C_y = (4 \text{ to } 5) \times 0.12 = 0.48 \text{ to } 0.6 \tag{7}$$

which conforms to the range suggested by the inelastic spectra of Fig. 4.

5. Structural system of the investigated building

The structure under investigation is a 3-storey reinforced concrete building in downtown Lefkada, located 200 m from shore, oriented at N135E (L) and N225E (T). The structure was designed in 1969, according to the 1954 Reinforced Concrete and the 1959 Seismic Codes. There is no information as to its condition and performance in the 1973 earthquake. It was hit severely by the 2003 earthquake, especially in the lower two floors. In the post-earthquake investigations the building was considered of high risk; it was abandoned and later demolished. A systematic post-earthquake investigation conducted by the authors provided as-built structural information and damage patterns. Blueprints were also made available to the authors by the owner.

The structural system consists of three 7-column frames connected with transverse beams at the ends, which form an elongated plan of dimensions 8.8 m by 31.2 m (Figs. 7(a), 7(b), 7(c)). The column dimensions vary with height and position in plan (Figs. 7, 8). The perimeter columns are 0.35 m × 0.35 m on the ground floor and reduce to 0.3 m × 0.3 m on the upper floors. The inner columns are larger, varying from 0.4 m × 0.4 m at ground floor to 0.35 m × 0.35 m at the upper floors. The lack of strong columns at the corners and the absence of concrete walls suggest a design focused on gravity loads - which is typical of the period.

The beams have cross sections varying from 0.25 m × 0.6 m to 0.2 m × 0.5 m with the inner beams being stronger than the outer. Concrete slabs are 0.15m thick in all floors with the exception of a large part of the first floor which is made out of wood.

According to blueprint information, the foundation consists of three strip footings of rectangular cross section located under the main frames, built without connecting beams. The outer footings have a cross section of 1 m × 0.5 m (Fig. 9) while the middle footing is 1.5 m × 0.5 m. Above the foundation there is a ground floor slab.

It is evident, both from field observations and blueprints, that concrete of C10 (B160) quality and steel reinforcement S220 were used, which was typical for small residential structures of the era. Examination of damaged columns suggests that stirrups were placed at intervals of 20 cm and were well closed which is judged as good construction by the standards of the time. It is apparent that more attention was put in the design and construction of beams following the practice of the 1970's in Greece.

Observed column damage was concentrated at the heads of columns on the first and second floor; severity varies from light (columns C1, C2, C21 of the 1st floor and C1, C6, C7, C8, C9, C10, C21 of the 2nd floor) to serious (C9, 1st floor and C2, C15, C19, C20, 2nd floor) as presented in Figs. 7(b), 7(c) (see also Figs. 10(a), 10(b)). Nevertheless no total member failures were observed, which can be attributed to sufficient ductility capacity of the columns versus the ductility demand.

Regarding the presence of infill walls, very few elements were used, as the structure had a commercial function. Where present, the infill walls were weak-having only one layer of bricks and there were large openings for the windows. Accordingly, their influence was neglected in this study.
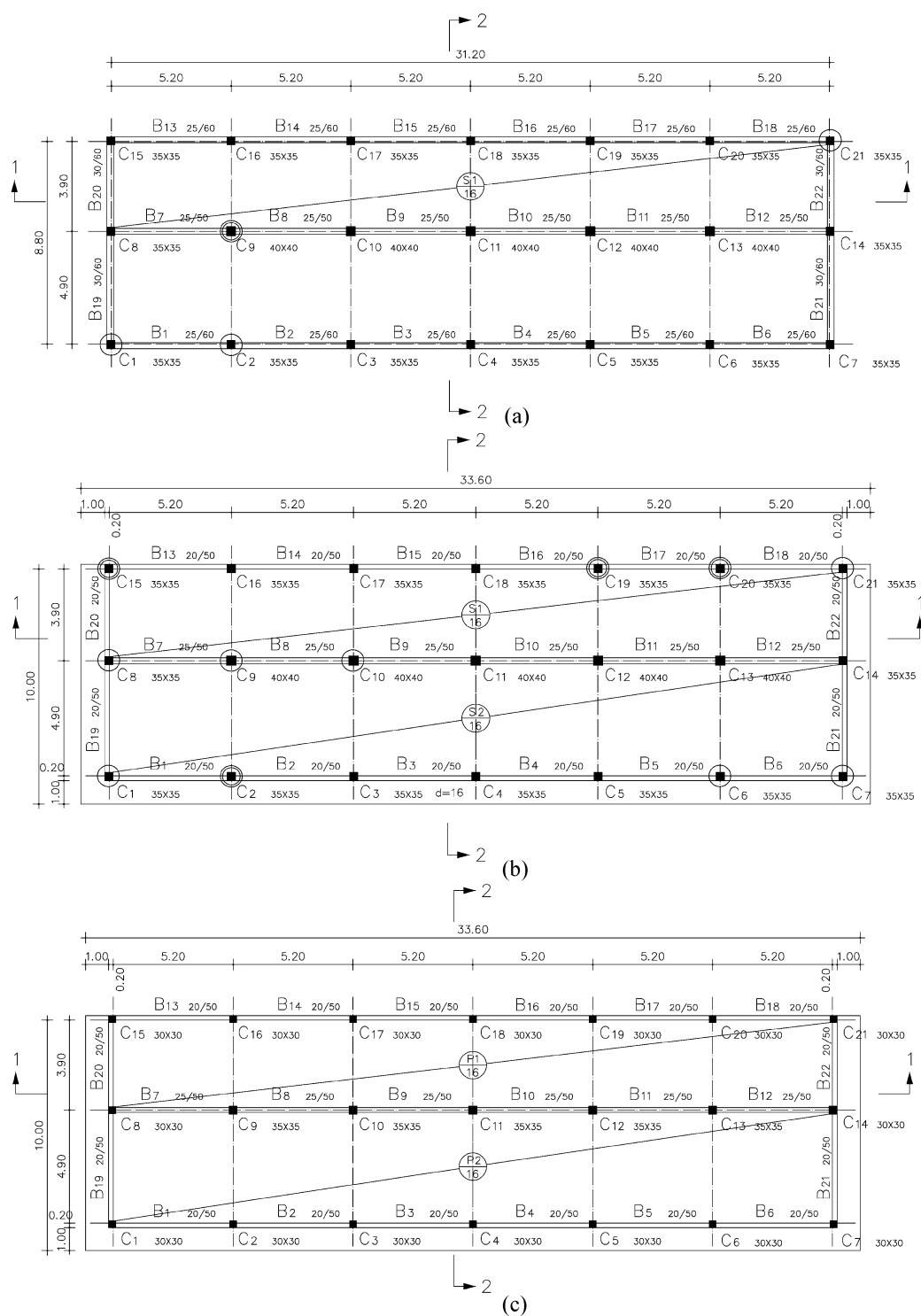
Fig. 7 Plan view: (a) 1st storey, (b) 2nd storey, (c) 3rd storey. Circle denote light cracks, Double circles denote serious cracks
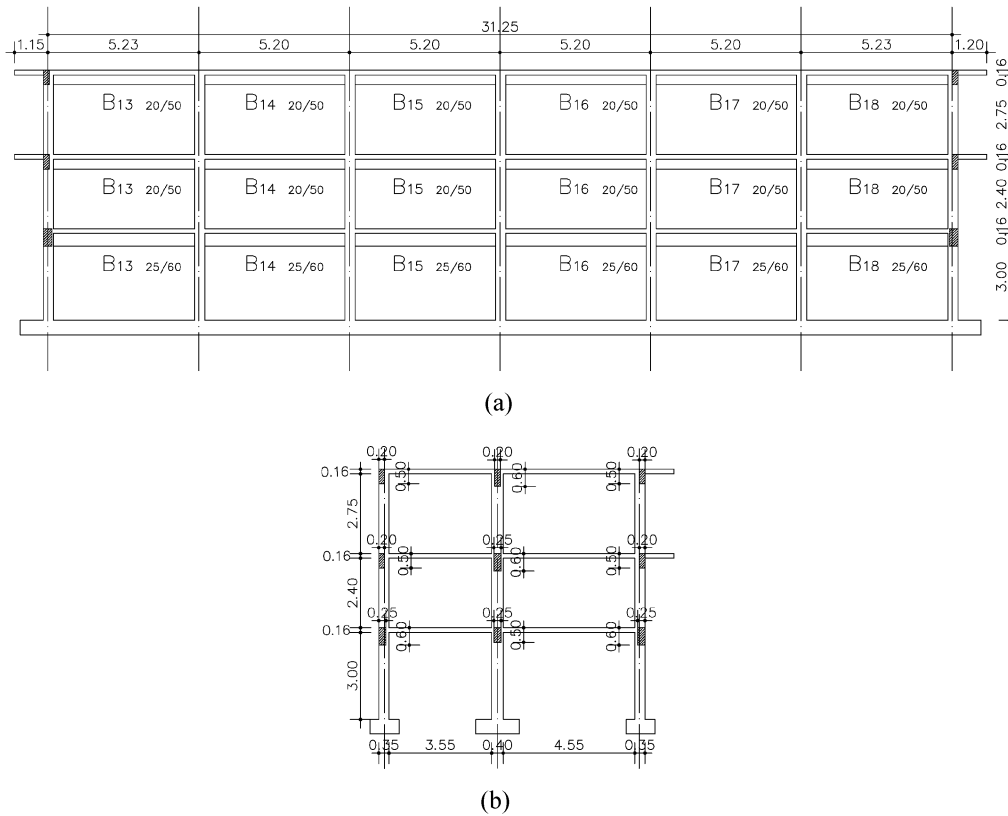
(a)

(b)

Fig. 8 Sections 1-1 (a) and 2-2 (b) of the building

6. Geotechnical conditions

Soil conditions in the town of Lefkada are among the softest encountered in Greece. Following the earthquake, a detailed geophysical and geotechnical exploration was conducted by KEDE (2003) based on SPT and Cross Hole tests, down to a depth of 30 meters.

The available data indicate the presence of a layer of stiff marl ($N_{SPT} > 50$), located at a depth of approximately 10-12 m, having shear wave velocity $V_{s,max} = 350$ m/s and thickness of over 20 m.
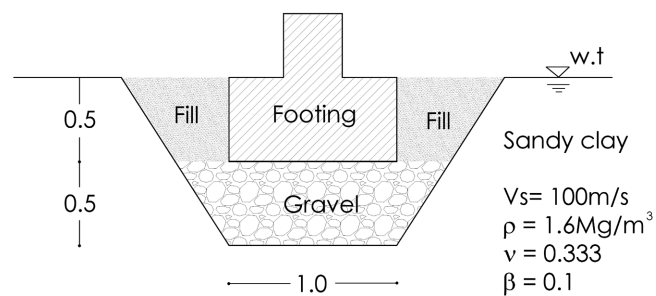

Fig. 9 Foundation properties

The overlying soil consists of soft alluvial deposits, primarily clayey sands and sandy silts, of $V_{s,max}$ less than 200 m/s. According to the Greek Seismic Code and EC8, these formations are classified as Soil Category C. Typical soil sections at the two locations are provided in Fig. 11. Apparently, the differences in S-wave velocities between the soil profiles are rather minor; it is possible that some of these discrepancies reflect limitations of the site exploration techniques. Our analyses of seismic

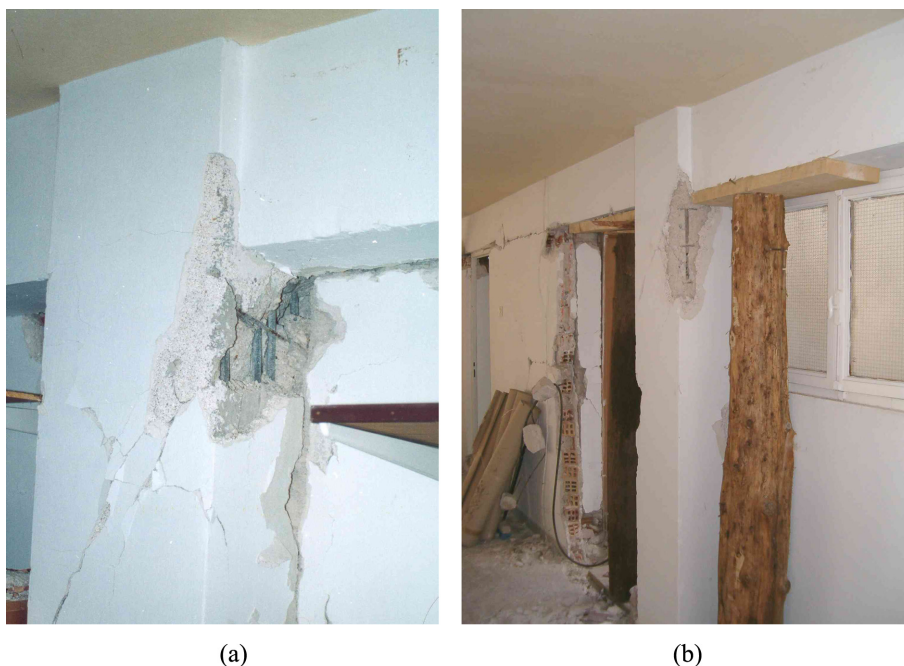(a)   (b)

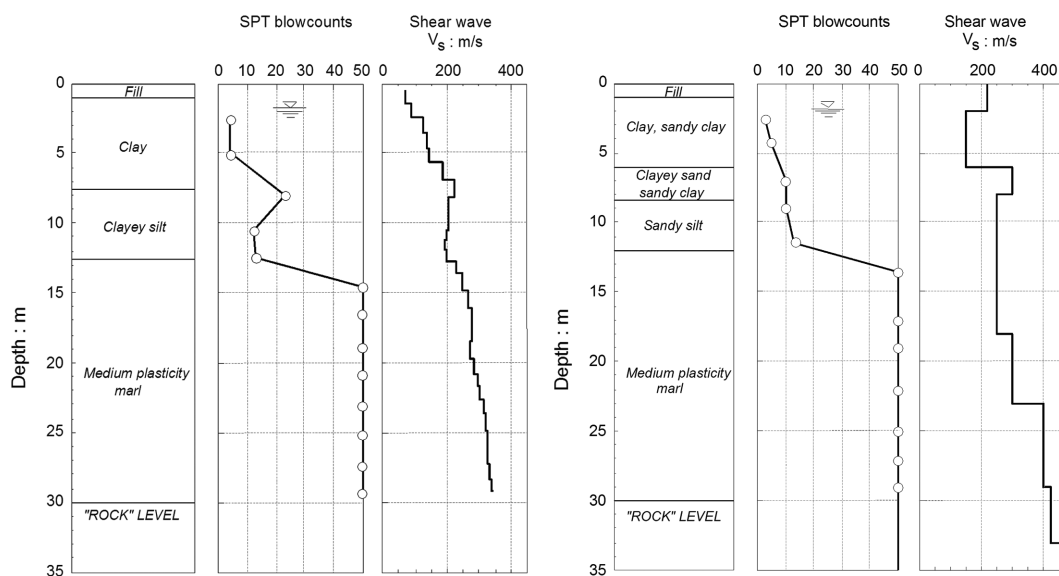Fig. 10 Serious cracks on columns K19 and K20, 2nd floor

Fig. 11 Soil profile and properties at (a) Lefkada Hospital station and (b) building site

soil-foundation interaction are based on values extracted from the borehole data of Fig. 11(b), which is the one closest to the building (20 m away).

Closed-form solutions of dynamic stiffness of spread footings have been derived by regression analysis based on finite- and boundary-element data. The validity of these expressions has been verified by several investigators over the years. Using the expressions recently published by Mylonakis *et al*. (2006), the soil data of borehole CX-1 in Fig. 11(b) (V_s = 100m/s, ρ_s = 1.6 Mg/m^3, v_s = 0.33), and the foundation properties in Fig. 9 i.e. foundation width $2B$ = 1 m, footing embedment D = 0.5 m, footing length $2L$ = 34 m distributed over seven footings, the stiffness of each footing can be approximated by

$$K_z = 51{,}000 \text{ KN/m}, \; K_y = 56{,}000 \text{ KN/m}, \; K_x = 49{,}000 \text{ KN/m} \tag{8}$$

$$K_{rx} = 125{,}000 \text{ KN m/rad}, \; K_{ry} = 735{,}000 \text{ KN m/rad} \tag{9}$$

Owing to small embedment, the cross-swaying-rocking stiffness of the footings can be ignored. Solutions for the dashpots acting in parallel to the footings were likewise obtained as

$$C_z = 2500 \text{ KN s/m}, \; C_y = 2400 \text{ KN s/m}, \; C_x = 2200 \text{ KN s/m} \tag{10}$$

$$C_{rx} = 130 \text{ KN m s}, \; C_{ry} = 160 \text{ KN m s} \tag{11}$$

The small values of the dashpot constants in the rocking modes are as expected.

7. Structural response simulations

A large set of simulations were performed on the structure. These include: (a) Response spectrum analyses to evaluate the design according to modern codes. (b) Pushover analyses intended to investigate the probable collapse mechanism and provide information as to strength and deformation capacities. (c) Non-linear time-history analyses for a more accurate evaluation of seismic demand.

7.1 Modeling

The structure is treated as a space frame subjected to combined gravitational and earthquake loading. The beam-column frame system is modeled with inelastic beam elements located along the centroidal axes of the members. With the exception of the wooden floor, slabs are considered undeformed in their own plane (diaphragms). Regarding the latter, elastic analyses using the computer code ETABS with and without considering diaphragm action were performed by the Authors. The structure fulfils the requirement of paragraph 4.3.1.(4) of EC8 stating that "The diaphragm is taken as being rigid, if, when it is modeled with its actual in-plane flexibility, its horizontal displacements nowhere exceed those resulting from the rigid diaphragm assumption by more than 10% of the corresponding absolute horizontal displacements in the seismic design situation". This, together with the lack of rotation of the slabs around a vertical axis) strengthens our confidence that the assumption of diaphragm action is valid.

Regarding gravitational loads, these were estimated according to the observations of the post-

earthquake investigation conducted by the authors. Apart from the dead loads of the building, a superimposed dead load of 2 KN/m^2 and a live load of 0.6 KN/m^2 were considered in all floors.

The analysis considers cracked properties for the members. Three different sets of properties were used: (a) properties according to Greek seismic code (OASP 2003) which consider stiffness equal to 50% of nominal (uncracked) values for beams and 100% of uncracked stiffness for the columns (to be referred hereafter as "full stiffness" case). This set of properties was used only in the response spectrum analysis with the purpose of investigating the adequacy of the design of the structure (b) Stiffness values at 20% and 30% of the uncracked for beams and columns respectively ("soft stiffness" case) as evaluated from the moment-curvature diagrams of the members. (c) Stiffness values at 50% and 70% of the uncracked for beams and columns respectively ("medium stiffness" case) which is close to EC8 suggestions and lie between (a) and (b).

Regarding the supports, two alternatives are considered: (a) fixed-base conditions and (b) flexible-base conditions. The simulations are performed using the computer codes ETABS 9.60 (Computers & Structures, Inc. 2009) and Rauomoko 3D (Carr 2005) which employ concentrated plasticity models.

7.2 Response spectrum analysis

The dynamic analysis considers the natural modes of the structure encompassing 90% of the total effective mass in each direction. For the analysis using full stiffness and for the fixed-base case, fundamental periods were estimated at 0.82 s along the transverse "weak" axis, and 0.58 s along the longitudinal "strong" axis of the building. For the flexible-base case, the periods were determined at 0.89 s and 0.6 s respectively (a 6% and 3% increase, respectively). As indicated by the long natural periods, the minor increase in period due to SSI and the strong participation of the first modes, the structure is indeed very flexible at ground level. Results for the two other sets of stiffness are presented in Table 4. It can be seen that the softest case, results in fundamental periods of 1.26 s and 1.03 s along the transverse and the longitudinal principal directions of the building, respectively.

As mentioned earlier, the structure was designed according to the 1959 Seismic Code - the first seismic regulations in Greece, which was based exclusively on pseudo-dynamic considerations. A constant distribution of the lateral load with a value of (εW) was considered, where ε is the seismic coefficient of the 1959 code and W is the gravity load of the structure. The equivalent demand in the realm of modern codes would be a constant response spectrum with $R_d = 1.75$ ($q \times \varepsilon$), 1.75

Table 4 Periods of the structure from various analyses employing different member stiffness and support conditions

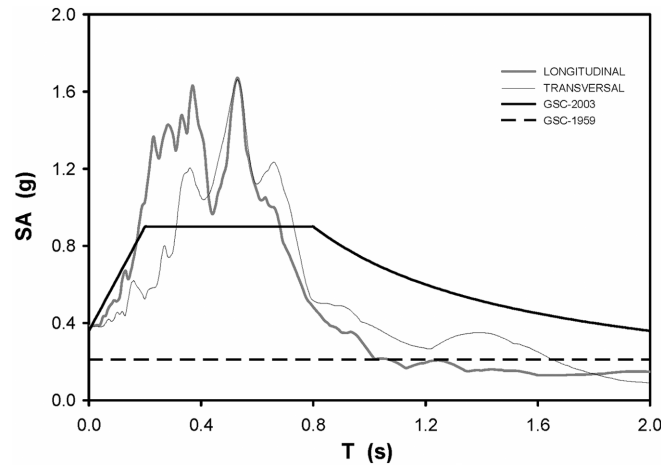| Model	Period (s)			
	1st mode (translational Y)	2nd mode (translational X)	3rd mode (translational Y)	4th mode (translational X)
Full stiffness	0.82	0.58	0.24	0.21
Full stiffness with SSI	0.88	0.60	0.24	0.21
Medium stiffness	0.89	0.66	0.26	0.23
Medium stiffness with SSI	0.95	0.69	0.26	0.23
Low stiffness	1.21	1.01	0.37	0.35
Low stiffness with SSI	1.26	1.03	0.37	0.35

Fig. 12 Acceleration spectra of Lefkada Hospital station oriented parallel to the L and T axes of the bulding compared to the Greek Seismic Code requirements

being an empirical conversion factor between modern and old codes, relating reinforced concrete provisions based on allowable stresses and ultimate strength concepts (Anagnostopoulos *et al.* 1987) and *q* is a behavior factor. Note, however, that the distribution of lateral loads in the two codes is not equivalent, as the modern one follows a "first mode" force distribution.

Should a value of 1.50 be adopted for the behavior factor (a reasonable approximation for old concrete structures) and factor ε taken at 0.08 as specified by the 1959 code for the region, then $R_d = 0.21$ which is shown as a horizontal broken line in Fig. 12.

Accordingly, the equivalent parameters in the realm of the Greek Seismic Code of 2003 would be: Seismicity $\alpha = 0.36$, importance factor $\gamma_I = 1$, ground type C, foundation factor $\theta = 1$, damping factor $\eta = 1$ (for $\zeta = 5\%$), $q = 1.5$ resulting in the response spectrum of Fig. 12.

These results from the analyses employing different support conditions show that the structure was rather underdesigned. There is an indication of failure in all corner columns, which comes as no surprise, for they were not carrying additional reinforcement - as they should have had by today's standards - compared to the inner columns.

7.3 Pushover analyses

The analyses were carried out in the longitudinal and the transverse directions of the structure, both for fixed-base and for flexible-base conditions. As mentioned in section 7.1 two different sets of stiffness values were considered, low stiffness and medium stiffness. The composite-spectrum technique recommended in ATC-40 (ATC 1996) was adopted in these analyses. Results are shown in Fig. 13.

On the basis of the nominal yield strength, V_{el}, and displacement, u_y, the overstrength factor, q_ω, of the building can be estimated from the relation

$$q_\omega = V_{max}/V_{el} \tag{12}$$

where V_{max} denotes the maximum force sustained. Given that the overall behavior factor q can be
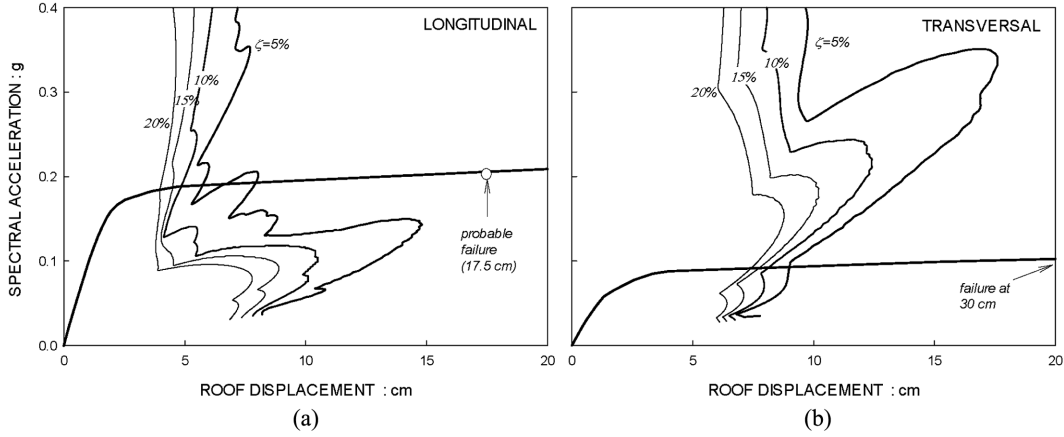
Fig. 13 Push-over diagrams and demand curves for the two orthogonal directions of the building

defined as a product of a ductility-related behavior factor, q_{μ}, and a structural overstrength factor, q_{ω}, one can write (BSSC 2000)

$$q = q_{\mu} \times q_{\omega} \tag{13}$$

Following ATC-40, the capacity curve is converted by dividing the horizontal load and roof displacements relatively to free-field by the a_1 and C_o coefficients, respectively, that account for the participation of the higher modes. For the structure at hand, using the pertinent values $a_1 = 0.86$ and $C_o = 1.3$, the capacity curves of Fig. 13 are obtained corresponding to the L and T direction of the building for the medium stiffness set.

Regarding the "strong" L direction (Fig. 13(a)), the base shear corresponding to the yield point is $V_{el} = 0.185W$ at a roof displacement of 1.9 cm. The failure point is located at $V_{max} = 0.206W$, at a roof displacement of 17.5 cm, providing a global overstrength $q_{\omega} = 1.10$. Plastic hinges start to develop at a roof displacement of approximately 4.8cm at certain columns of the 1st and 2nd storey, including the ones that were actually damaged. Note that in most cases, formation of plastic hinges is related to reduction of the cross-section of the columns at the slab separating the 2nd and 3rd floors. As can be seen from Fig. 13(a), seismic demand in this direction is about 4 to 5 cm, which suggests permanent damage but no collapse.

With reference to the "weak" T direction, base shear corresponding to the elastic point is $V_{el} = 0.086W$ at a roof displacement of 1.7 cm, whereas failure point is located at $V_{max} = 0.11W$, at a displacement of 30 cm. This results in a system ductility capacity, $\mu^{(T)} = 30/1.7 = 19$ and an overstrength $q_{\omega} = 1.3$. Plastic hinges start to appear at a displacement of 15 cm. As can be derived from Fig. 13(b), seismic demand in this direction is 9 cm, thus obviously, at this point there is also permanent damage.

The above simplified analysis shed light on the behavior of the structure. Accepting, as a reasonable assumption, the equal displacement rule (Veletsos and Newmark 1960), the required strength to survive the imposed motion along the L direction would be

$$C_y^{(L)} = \frac{SA(0.6s)}{\mu_c^{(L)}q_{\omega}g} = \frac{1.05g}{9 \times 1.1 \times g} = 0.11 \tag{14}$$

Similarly, for the *T* direction

$$C_y^{(T)} = \frac{SA(0.89s)}{\mu_c^{(T)} q_\omega g} = \frac{0.4g}{19 \times 13 \times g} = 0.016 \tag{15}$$

Apparently, along *T* direction, the structure employs only a small fraction (of the order of 15%) of its "design strength" of 0.11W, whereas along the *L* direction it uses over 50% of its design strength of 0.21W. Naturally, this difference would be reflected in deformations, hence the more pronounced damage observed in the longitudinal direction. This feature is also indicated in direct displacement analysis using the composite spectra of Fig. 13. Indeed, for conservative estimates of roof displacement demand at 5 cm and 7.5 cm, respectively, along the *L* and *T* directions, the associated global ductility demands are

$$\mu^{(L)} = \frac{5\text{cm}}{1.9\text{cm}} = 2.6 \tag{16}$$

and

$$\mu^{(T)} = \frac{7.5\text{cm}}{1.7\text{cm}} = 4.7 \tag{17}$$

This is a surprising outcome, as the less affected direction *T* develops almost twice the ductility demand developed in the severely hit *L* direction. However, comparisons of these values with corresponding global capacities of 9 and 19 respectively, show that the mobilization of ductility capacity in the *T* direction is less than in the *L* direction (29% and 25% respectively), although the difference is much smaller than the mobilization of the corresponding "design strengths". It is noteworthy that at response displacements of 5 cm and 7.5 cm, no member fails in the *T* direction - despite the existence of several plastic hinges, whereas, at the same roof displacement several members fail in the *L* direction. In summary, the above difference in ductility demand in the two orthogonal directions is due mainly to the difference in the corresponding yield strengths (0.11 versus 0.21) not that in elastic force demand.

It should be noticed that the above pushover analysis invariably shows development of plastic hinges at the base of columns on the ground floor. Such a behavior was not observed in the post-earthquake investigations although no inspection was attempted below the ground floor slab.

Conclusions from the analyses employing the soft set of stiffness lead to similar conclusions.

7.4 Nonlinear time-history analyses

To develop additional insight on the performance of the structure, non-linear time history analyses were performed, both for fixed-base and flexible-base conditions. As mentioned in section 7.1 two different sets of member stiffness were considered, the ones referred to as "low stiffness" and "medium stiffness". Both elastic and inelastic analyses were conducted. To this end, the horizontal components of the Hospital station recording were rotated 70° clockwise to conform to the orthogonal directions of the structure.

In order to check if dynamic response along the *L* and *T* directions is coupled, analyses with excitation only in the *L* or *T* direction were considered. It was shown that dynamic response along *L* and *T* directions is practically uncoupled as expected from the symmetry of the structure. This trend

becomes more pronounced for inelastic conditions.

Elastic and inelastic displacements are comparable in all cases. Peak displacements at the top floor in the transverse direction vary from 0.10 m for medium stiffness with no SSI to 0.12 m for low
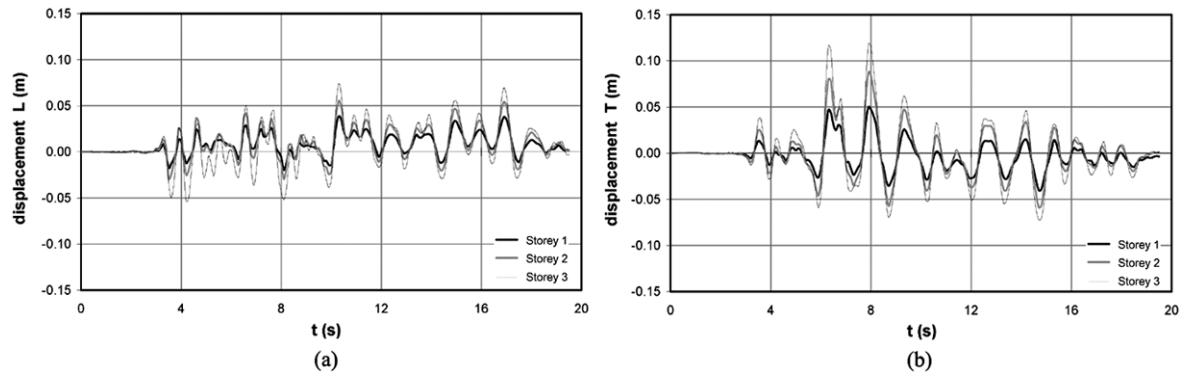

Fig. 14 Displacements at L and T direction of all floors, on top of damaged column 20, from the "soft set" of calculations (low member stiffness with SSI)
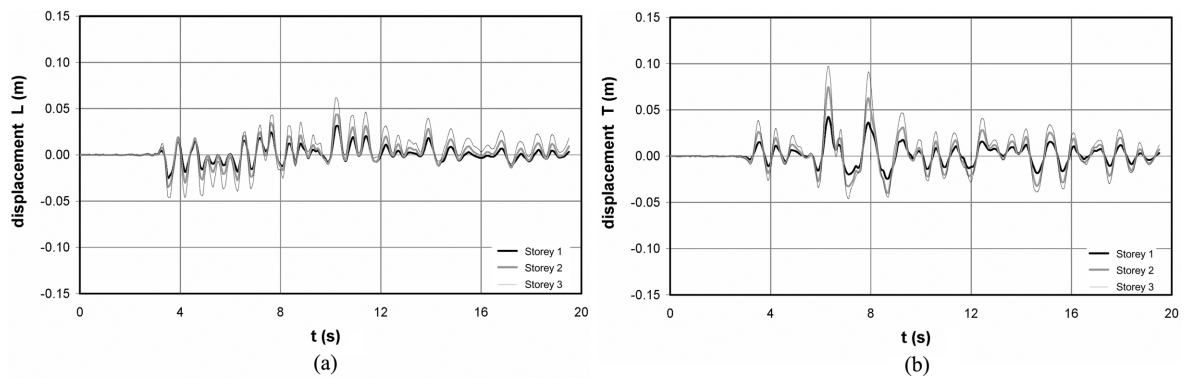

Fig. 15 Displacements at L and T direction of all floors, on top of damaged column 20, from the "medium stiffness set" of calculations (medium member stiffness without SSI)
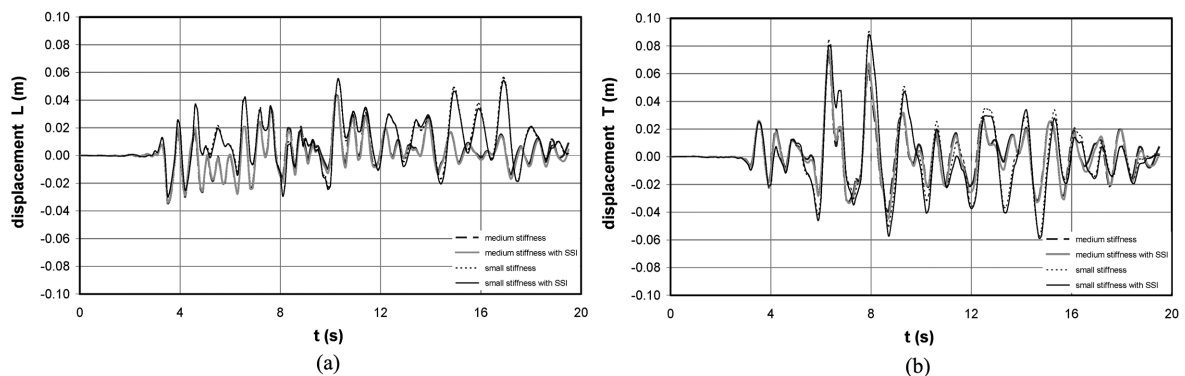

Fig. 16 Comparison of displacements on top of column 20 on second floor from various analyses with different structural properties and support conditions
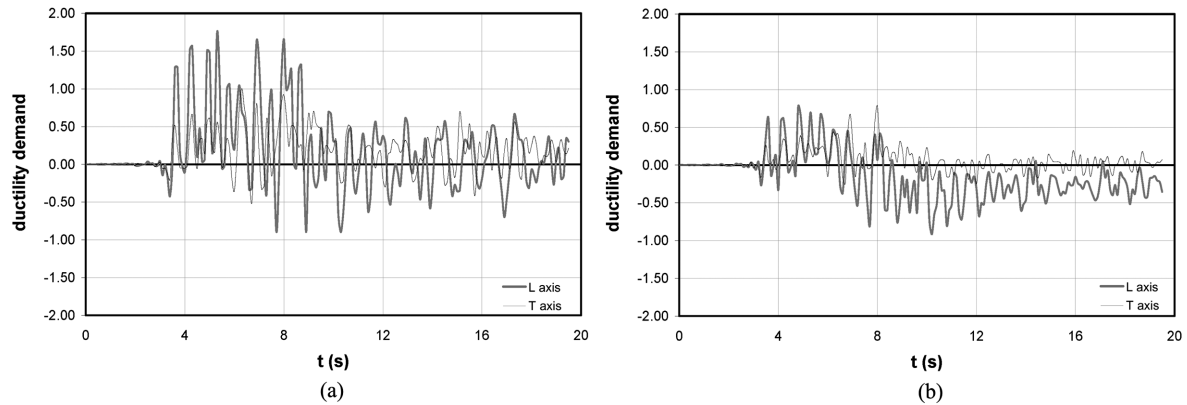
Fig. 17 Rotational ductility demand on top of column 20 on second floor for the softest (low member stiffness with SSI) and the stiffest (medium member stiffness without SSI) sets of calculations

stiffness with SSI. In the longitudinal direction the range is from 0.062 m to 0.075 m respectively. Figs. 14 and 15 present the displacements for each storey of column 20 - one that was severely damaged - for the softest (low stiffness with SSI) and the stiffest (medium stiffness without SSI) set of calculations. Fig. 16 presents a comparison of displacements of the top of column 20 on second floor.

In all members that failed, the ductility demand exceeded the yield point of the cross section. In general, ductility demand in the longitudinal direction is higher than that in the transversal direction, which is the opposite to that observed in the previous section. Note, however, that the specific ductility demand is local, expressed in terms of member rotations, as opposed to global, expressed in terms of roof translations. This difference is more clear in the members that failed.

In Figs. 17(a) and 17(b) ductility demand on top of column 20 for the softest (low stiffness with SSI) and the stiffest (medium stiffness without SSI) sets of calculations is presented. Evidently, as the structure gets softer the ductility demand increases. It should be mentioned that the softer set of calculations probably represents the more realistic case, taking into account both the actual cracked member stiffness and the soil-structure interaction effect.

8. Conclusions

The main conclusions of this study are:
(1) Peak recorded ground motions were unusually strong, with effective accelerations exceeding 0.5 g, and peak spectral accelerations exceeding 2.2 g at a period of 0.53 s.
(2) Ground motion in the town of Lefkada (10 km from the fault) was stronger in the fault-parallel than in the fault-normal direction. This could be attributed, among other reasons, to backward source directivity resulting from the location of the station relative to the rupture, and the rupture mechanism.
(3) Structural damage in the area was surprisingly low. This can be attributed to the low weights of the low-rise traditional structures on the island, built using an ingenious combination of masonry and wood. Back-calculated yield seismic coefficients for these structures are estimated at 0.5 to 0.6.
(4) The structure under investigation was quite unusual, exhibiting 50% longer period and 100%

lower strength in the transverse than in the longitudinal direction. The difference in period is partly due to SSI, triggered by the very soft soil conditions ($V_{s,max}$ = 150 m/s), in conjunction with the lack of transverse beams in the foundation. This increase in period due to SSI is approximately 3% and 6% in the longitudinal and the transverse directions respectively.

(5) Despite the stronger displacement response and higher global ductility demand (by a factor of 2) along the "weak" direction of the building, column damage occurred along the "strong" longitudinal direction. This counterintuitive behavior is attributed to the high ductility capacity (of about 20 or so) available in the transverse direction.

(6) Simplified push-over analyses provided fair estimates of building response and global ductility expressed in terms of translations.

(7) Non-linear dynamic analyses showed that the peak roof displacement in the longitudinal direction was lower (by approximately 40%) than that of the transversal whereas the member ductility demand was higher which is consistent with the damages that occurred.

(8) Soil-structure interaction increased the ductility demand by a small amount. Had the structure been stiffer this effect would have been more pronounced.

(9) Despite some discrepancies in the distribution of damages the analyses provided results in accordance to the post-earthquake investigation.

Acknowledgments

References

Anagnostopoulos, S., Rinaldis, D., Lekidis, V., Margaris, V. and Theodoulidis, N. (1987), "The Kalamata, Greece, earthquake of September 13, 1986", *Earthq. Spectra*, **3**, 365-402.

ATC (1996), "Seismic evaluation and retrofit of concrete buildings", ATC 40, Vol 1.

Bouckovalas, G.D. and Papadimitriou, A.G. (2003), "Lefkada M=6.4, 14/8/03 earthquake: analysis of soil effects and liquefaction on strong seismic motion recordings", *Proceedings 1st International Workshop on Earthquake Prediction Research*, Special Session, Athens.

Benetatos, C., Kiratzi, A., Roumelioti, Z., Stavrakakis, G., Drakatos, G. and Latoussakis, I. (2005), "The 14 August 2003 Lefkada Island (Greece) earthquake: focal mehanisms of the mainshock and of the aftershock sequence", *J. Seismol.*, **9**, 171-190.

Benetatos, C., Dreger, D. and Kiratzi, A. (2007), "Complex and segmented rupture associated with the 14 August 2003 (Mw 6.2) Lefkada (Ionian Islands) earthquake", *B. Seismol. Soc. Am.*, **97**(1B), 35-51, doi: 10.1785/ 0120060123.

Building Seismic Safety Council (2000), *NEHRP recommended provisions for the development of seismic regulations for new buildings and other structures*, D.C.

Carr, A. (2005), *Ruaumoko 3D*, University of Canterbury, Christchurch, New Zealand.

Computers & Structures, Inc. (2009), *ETABS 9.6.0 - Integrated Building Analysis & Design*.

Earthquake Planning & Protection Organization [OASP] (2003), *Greek seismic code*, Athens-Greece, 72pp.

Eurocode-2 (2001), *Design of concrete structures*, prEN 1992-1, CEN Brussels.

Eurocode-8 (2002), *Design of structures for earthquake resistance*, prEN 1998-1, CEN Brussels.

Gazetas, G. (2004), "Geotechnical aspects of the Ms 6.4 Lefkada Island, Greece, 2003 earthquake: preliminary assessment", *Proc, Fifth International Conference on Case Histories in Geotechnical Engineering*, New York.

Giarlelis, C., Kostikas, C. and Plakas, A. (2003), "Seismic behavior of a multi-storey RC building that collapsed during the 1999 Athens Earthquake", *FIB - Symposium on Concrete Structures in Seismic Regions*, Athens.

Giarlelis, C., Lekka, D., Mylonakis, G., Anagnostopoulos, S., Karabalis, D. and Vgenopoulou, I. (2006), "Performance of a 3-storey R/C structure on soft soil in the M6.4 Lefkada, 2003, Greece, earthquake", *1st European Conference on Earthquake Engineering and Seismology*, Geneva.

Institute for Engineering Seismology and Aseismic Structures [ITSAK] (2004), *The Lefkada (M = 6.2) earthquake*, August 14 2003: strong ground motion and consequences on the built and non-built environment", Technical Chamber of Greece, 78p. (in Greek)

Karakostas, C., Lekidis, V., Makarios, T., Salonikios, T. Issam S. and Demosthenous, M. (2005), "Seismic response of structures and infrastructure facilities during the Lefkada, Greece earthquake of 14/8/2003", *Eng. Struct.*, **27**, 213-227.

Karakostas, V., Papadimitriou, E. and Papazachos, C. (2004), "Properties of the 2003 Lefkada, Ionian Islands", Greece, Earthquake Seismic Sequence and Seismicity Triggering, *B. Seismol. Soc. Am.*, **94**(5), 1976-1981.

KEDE (2003), *Results of geophysical and geotechnical exploration in Lefkada island*, Athens.

Margaris, B., Papaioannou, C., Theodulidis, N., Savaidis, Anastasiadis, A., Klimis, N., Makra, K., Demosthenous, M., Karakostas, C., Lekidis, V., Makarios, T., Salonikios, T. and Sous, S. *et al.* (2003), *Preliminary observations on the August 14, 2003, Lefkada Island (Western Greece) earthquake*, EERI Special Earthquake Report, 12p.

Mavroeidis, G.P. and Papageorgiou, A. (2000), "Analysis and simulation of the near – source motion recorded at aigion during the Ms = 6.2, June 15, 1995 aigion earthquake (Greece)", *Sixth International Conference on Seismic Zonation: Managing Earthquake Risk in the 21st Century*, Proc., EERI, Oakland.

Mylonakis, G., Nikolaou, S. and Gazetas, G. (2006), "Footings under dynamics loads: analysis and design issues with emphasis on bridge foundations", *Soil Dyn. Earthq. Eng.*, **26**(9), 824-853.

Mylonakis, G., Voyagaki, E. and Price, T. (2003), "Damage potential of the 1999 Athens, Greece, accelerograms", *B. Earthq. Eng.*, **1**(2), 205-240.

Papadopoulos, G., Karastathis, V., Ganas, A., Pavlides, S., Fokaefs, A. and Orfanogiannaki, K. (2003), "The Lefkada, Ionian Sea (Greece), shock (Mw 6.2) of 14 August 2003: evidence for the characteristic earthquake model from seismicity and ground failures", *Earth Planets Space*, **55**, 713-718.

Papazachosm, B. and Papazachou, K. (1997), *The earthquakes of Greece*, pub. Ziti, 304p.

Rondoyannis P. (1997), *The seismicity of Lefkada (1469-1971)*, Annals no 8, Society for Lefkadian Studies.

Sextos, A., Katsanos, E. and Manolis, G. (2010), "EC8-based earthquake records selection procedure evaluation: validation study based on observed damage of an irregular R/C building", *Soil. Dyn. Earthq. Eng.*, Corrected Proof, Available online 18 December 2010, ISSN 0267-7261, DOI: 10.1016/j.soildyn.2010.10.009.

Skarlatoudis, A.A., Papazachos, C.B., Margaris, B.N., Theodoulidis, N., Papaioannou, C.H., Kalogeras, I., Scordilis, E.M. and Karakostas, V.G. (2003), "Empirical peak ground motion predictive relations for shallow earthquakes in Greece", *B. Seismol. Soc. Am.*, **93**, 2591-2603.

Spyropoulos, P.I. (1997), *Chronicle of Greek earthquakes*, pub. Dodoni, 453p. (in Greek)

Veletsos, A.S. and Newmark, N.M. (1960), "Effect of inelastic behavior on the response of simple system to earthquake motion", *Proc. 2nd World Conference on Earthquake Engineering*, Tokyo, p. 895-912.

Zahradnik, J., Serpetsidaki, A., Sokos, E., Tselentis, G. (2005), "Iterative deconvolution of regional waveforms and a double-event interpretation of the 2003 Lefkada earthquake, Greece", *B. Seismol. Soc. Am.*, **95**(1), 159-172.

SA